Proceedings of the
International Conference on Mechanical Engineering 2011
(ICME2011) 18-20 December 2011, Dhaka, Bangladesh

ICME11-FL-004

EFFECTS OF SWIRL IMPARTED AT INLET ON THE RECIRCULATION BUBBLE GENERATED IN THE TURBULENT FLOW IN AN AXI-SYMMETRIC SUDDEN EXPANSION

Snehamoy Majumder, **Debajit Saha, Arindam Mandal and Vikram Roy**

Department of Mechanical Engineering, Jadavpur University, Kolkata-700032, India.

ABSTRACT

The turbulent fluid flow through an axi-symmetric sudden expansion is a general phenomenon associated with the expansion flows in the pipe lines, dump combustor chamber etc., where in general the recirculation bubbles are generated. In case of combustion chambers swirl promotes extensive mixing of the fuel and air and thereby increases the combustion efficiency with the augmentations of the strong radial flow. In the present study the numerical analysis of the turbulent fluid flow through an axi-symmetric sudden expansion with the swirl present at the inlet has been carried out by using modified $k-\varepsilon$ turbulence model. The streamline contour and vector plots have been presented to illustrate the effects of the variation of the swirl number on the size and strength of the recirculation bubble. A correlation has been obtained between the reattachment length and the inlet swirl angle to analyze the effects swirl.

Keywords: Sudden Expansion, Recirculation Bubble, Reattachment Length, Swirl.

1. INTRODUCTION

Turbulence is the most common state of fluid motion. The turbulent fluids flows through sudden expansion passage have both fundamental scientific interest and numerous practical applications. The engineering applications such as the separated flow associated with pipelines, dump combustors, different ducting devices etc. are examples of the turbulent flow through the sudden expansion. To improve the performance of such applications, an accurate description of the flow patterns are required. The turbulent flow in such devices is very complicated owing to generation of recirculation bubble and thereby changing the downstream flow structures. The swirling flow is of immense significance in the combustion chambers. The purpose of the swirl is to assist in the creation of the toroidal flow reversal to obtain the higher rate of mixing. The recirculation zone is an adverse pressure gradient region. This phenomenon of adverse pressure gradient creates high turbulent fluctuation. Therefore the turbulent mixing and combustion are benefited when the recirculation zones are formed in the combustors. The recirculation obtained due to the swirl provides better mixing. Because of the inherent importance of swirling flow in many engineering applications, their investigations have been the subject of continued interest among the fluid mechanics researchers. In the present analysis the effect of the swirl in the downstream of the flow field has been observed.

During the last five decades the turbulent fluid flow through the sudden expansion passage for both swirl and without swirl condition has been rigorously investigated by the researchers throughout whole world. Talbot [1] was first to investigate the laminar swirling flow in the pipe. Chaurvedi [2] first analyzed the flow characteristics in the axi-symmetric expansion. The effects of the sudden expansions and compressions on the turbulent boundary layer were presented by White [3]. The turbulent flow in the downstream of the rearward facing step was experimentally analyzed by Etheridge *et al.* [4]. Their turbulence measurements revealed the development of new shear layer, which splits at reattachment with about one-sixth of the mass flow deflected in the upstream. Their results indicated that near the wall the length scales increases more rapidly with distance from the wall than in an attached boundary layer. Habib *et a.l* [6] numerically simulated the flow and heat transfer of the swirling turbulent flow behind the sudden expansion pipe. They predicted that with the increase in the maximum Nusselt number the swirl number increases.

Lilley *et al.* [7] presented the Five-hole pitot tube probe time-mean velocity measurements for the confined swirling flows. Both the non-reacting swirling and non swirling flows were investigated in the axi-symmetric test section with an expansion ratio of 2. They observed that the non-swirling confined jet possessed the corner recirculation zone with no central recirculation zone. The

presence of the swirler shortens the corner recirculation zone and generates a central recirculation zone followed by a precessing vortex core. The experimental analysis of the flow with the swirl in the circular duct was presented by Aoki *et al.* [8]. The velocity and the turbulence of the swirling flow in the circular duct were measured by using the Laser Doppler Velocimeter (LDV). They illustrated the characteristics of the turbulent intensity, Reynolds stress, turbulent energy and turbulent dissipation ratio for the different swirl numbers. Hallet [9] presented the model for estimating the minimum or critical swirl intensity required to produce central recirculation in a swirling sudden expansion flow. The results from their proposed model showed that the swirl required for the central recirculation could be reduced by producing an inlet flow with the small solid body core or a velocity deficit on the axis. A momentum integral model was developed by Hallet *et al.* [10] to predict the size and the maximum recirculating mass flow rate for the central recirculation produced by swirling flow in a sudden expansion. Their results showed that with all other things being equal the recirculation rate increases linearly with inlet swirl intensity and expansion ratio. The numerical simulation of the turbulent flow with inlet swirl in the axi-symmetric sudden expansion was presented by Guo *et al.* [11]. They proposed that the precessing vortex core was an inherent characteristic of the swirling flow inside the axi-symmetric sudden expansion.

The features of the swirling flow in sudden expansion were experimentally described by Palm *et al.* [12]. The velocity profile and the velocity gradient in the annular cross section were measured by using the Laser Doppler technique. They proposed that the axial velocity profile became increasingly asymmetric with increased swirl intensity. Vanierschot *et al.* [13] theoretically studied the influence of swirl on the reattachment length in an axi-symmetric sudden expansion. An analytical expression was derived by them to predict the influence of swirl on the reattachment length in an axi-symmetric sudden expansion. It was proposed by them that the reattachment length depends on the swirl number and the expansion ratio.

In the present study the attention is mainly focused on determining the effects of the swirl imparted at inlet on the recirculation bubble generated due to the turbulent fluid flow through the sudden expansion passage. A correlation between the recirculation bubble length and inlet swirling angle has been developed. The radial distribution of axial velocity has also been analyzed. The control volume formulation of Patankar with SIMPLER algorithm and power-law scheme has been employed for the computational analysis.

2. GEOMETRICAL DESCRIPTION

In figure 2.1 the flow geometry has been shown in the cylindrical coordinate system with $r - x$ axes. The geometry of the considered problem is symmetric with the x-axis. Here the swirling condition has been taken into consideration. The flow at the inlet of the passage is along the axial direction. In the above figure the inlet axial velocity has been indicated as U_{in}.

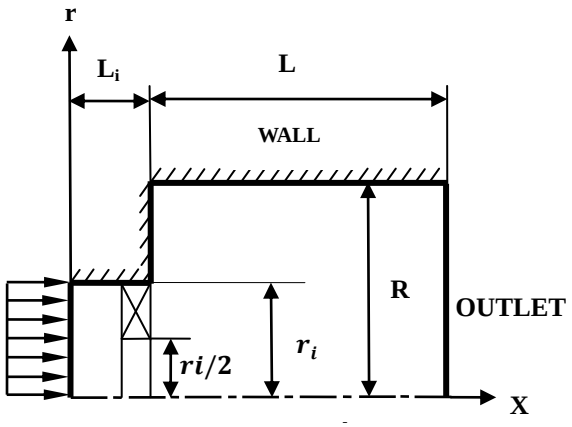

Fig 1. Schematic diagram of the flow through axi-symmetric sudden expansion with swirl.

The axial inlet velocity is 15 m/s. The inlet velocity remains constant throughout the analysis process. The swirl is imparted from the inlet of the passage. For the analysis the swirl number is varied. The variation of the swirl number is obtained by varying the inlet swirl angle. The inlet swirl angle is varied from 0° to 75°. The upstream length of the duct is represented as L_i. The value of L_i is taken as 0. 04 m. The downstream length of the duct is represented as L. The value of the downstream length of the duct is 0.75 m. Both the upstream and downstream length remains constant throughout the analysis. In the above figure the radius of the duct at the upstream is represented by r_i. The value of the upstream radius remains constant and it is 0.03125 m. The radius of the swirler is half of the radius of the passage at the upstream. The radius of the swirler taken for the analysis is 0.015625 m. The downstream radius of the circular passage is denoted by R and its value is taken as 0.0625 m. The value of the geometrical parameters remains constant throughout the analysis. The expansion ratio for this geometrical model is 2.

3. GOVERNING EQUATIONS

In the present analysis the considered steady, incompressible, turbulent flow is modeled by the momentum and continuity equations.

3.1 Continuity Equation

$$\frac{\partial(\rho\bar{u})}{\partial x}+\frac{1}{r}\frac{\partial(\rho r\bar{v})}{\partial r}=0$$

3.2 Momentum Equations

Axial Component (x-component):

$$\rho\left[\bar{v}\frac{\partial\bar{u}}{\partial r}+\bar{u}\frac{\partial\bar{u}}{\partial x}\right]=-\frac{\partial\bar{p}}{\partial x}+\frac{\partial}{\partial x}\left(\mu_{eff}\frac{\partial\bar{u}}{\partial x}\right)+\frac{1}{r}\frac{\partial}{\partial r}\left(r\mu_{eff}\frac{\partial\bar{u}}{\partial r}\right)+\left[\frac{\partial}{\partial x}\left(\mu_{eff}\frac{\partial\bar{u}}{\partial x}\right)+\frac{1}{r}\frac{\partial}{\partial r}\left(r\mu_{eff}\frac{\partial\bar{v}}{\partial x}\right)\right]$$

Radial Component (r-component):

$$\rho\left[\bar{v}\frac{\partial\bar{v}}{\partial r}+\bar{u}\frac{\partial\bar{v}}{\partial x}\right]=-\frac{\partial\bar{p}}{\partial r}+\frac{\partial}{\partial x}\left(\mu_{eff}\frac{\partial\bar{v}}{\partial x}\right)+\frac{1}{r}\frac{\partial}{\partial r}\left(r\mu_{eff}\frac{\partial\bar{v}}{\partial r}\right)+\left[\frac{\partial}{\partial x}\left(\mu_{eff}\frac{\partial\bar{u}}{\partial r}\right)+\frac{1}{r}\frac{\partial}{\partial r}\left(r\mu_{eff}\frac{\partial\bar{v}}{\partial r}\right)\right]-2\mu_{eff}\frac{\bar{v}}{r^2}+\rho\frac{\bar{w}^2}{r}$$

Where, $\bar{u}$ *and* $\bar{v}$ are the mean velocity components along x and r directions respectively.
The effective viscosity is,

$$\mu_{eff}=\mu_l+\mu_t$$

Where, μ_l and μ_t are molecular or laminar viscosity and eddy or turbulent viscosity respectively.
Equation (1), (2) and (3) are governing equations for describing the mean flow characteristics of a turbulent flow.
The eddy viscosity is given by,

$$\mu_t=\rho C_\mu k^2/\varepsilon$$

Where C_μ is an empirical coefficient.
The modification of the empirical constant is given by,

$$C_\mu=\frac{-K_1K_2}{\left[1+8K_1{}^2\frac{k^2}{\varepsilon^2}\left(\frac{\partial U_S}{\partial n}+\frac{U_S}{R_C}\right)\frac{U_S}{R_c}\right]}$$

Here, $U_S=\sqrt{\bar{u}^2+\bar{v}^2}$
R_C is the radius of curvature of the concerned streamline ($\psi=$ constant). The values of K_1 and K_2 are taken as 0.27and 0.3334 respectively.

3.3 Turbulence $\kappa-\varepsilon$ Model

The $\kappa-\varepsilon$ equations are given by,
$\kappa-$Equation:

$$\rho\left[\bar{u}\frac{\partial k}{\partial x}+\bar{v}\frac{\partial k}{\partial r}\right]=\frac{\partial}{\partial x}\left[\left(\mu_l+\frac{\mu_t}{\sigma_k}\right)\frac{\partial k}{\partial x}\right]+\frac{1}{r}\frac{\partial}{\partial r}\left[r\left(\mu_l+\frac{\mu_t}{\sigma_k}\right)\frac{\partial k}{\partial r}\right]+\rho G-\rho\varepsilon$$

Where, G is the production term and given by:

$$G=\mu_t\left[2\left\{\left(\frac{\partial\bar{v}}{\partial r}\right)^2+\left(\frac{\partial\bar{u}}{\partial x}\right)^2+\left(\frac{\bar{v}}{r}\right)^2\right\}+\left(\frac{\partial\bar{u}}{\partial r}+\frac{\partial\bar{v}}{\partial x}\right)^2\right]$$

$\varepsilon-$Equation:

$$\rho\left[\bar{u}\frac{\partial\varepsilon}{\partial x}+\bar{v}\frac{\partial\varepsilon}{\partial r}\right]=\frac{\partial}{\partial x}\left[\left(\mu_l+\frac{\mu_t}{\sigma_\varepsilon}\right)\frac{\partial\varepsilon}{\partial x}\right]+\frac{1}{r}\frac{\partial}{\partial r}\left[r\left(\mu_l+\frac{\mu_t}{\sigma_\varepsilon}\right)\frac{\partial\varepsilon}{\partial r}\right]+C_{\varepsilon1}G\frac{\varepsilon}{k}-C_{\varepsilon2}\frac{\varepsilon^2}{k}$$

Here, $C_{\varepsilon1}, C_{\varepsilon2}, \sigma_k$ and σ_ε are the empirical turbulence constants, and some typical values of these constants in the standard *k*-ε model are recommended by Launder and Spalding [14] which are given below-

$C_{\varepsilon1}$ = 1.44
$C_{\varepsilon2}$ = 1.92
σ_k = 1.0
σ_ε = 1.3

The final discretized equations have been solved by applying the uniform grid system with 251 × 151 points. It was observed that the results converge at lesser grid points than this grid system, however for the sake of any unwanted instability the present work has been done with a grid system of above mentioned value. It has been observed that the grid independent study has shown 0.001% change in the stream wise velocity. The results of the present analysis calculated by employing the uniform grid system are compared with the benchmark numerical results obtained by applying the non-uniform grid system and it is found to be satisfactory.

3.2 The Swirl Number

The degree of the influence of swirling flow is usually characterized by the swirling number, which is a non-dimensional number. The swirl number is the ratio between the axial fluxes of the swirl momentum to the axial flux of the axial momentum.

$$S=\frac{\int_0^R\bar{U}\bar{W}r^2dr}{R\int_0^R\bar{U}^2rdr}$$

Where, R is the radius of the pipe at different axial positions. $\bar{U}$ and $\bar{W}$ are the mean axial and tangential velocity components, respectively.

4. BOUNDARY CONDITIONS

The governing equations by themselves do not yield solution to the given problem. Therefore additional boundary information is required at the inlet, outlet, the axis and the solid wall. The boundary conditions are as follows,

At the Inlet:-
(a) The inlet axial velocity is uniform. (U_{in}= Constant)
(b) The tangential velocity $W_{in}= U_{in}\tan\boldsymbol{\theta}$.
(c) Fully developed velocity profile has been taken at the inlet.
(d) The turbulence energy and dissipation rate are taken as:

$$k_{in}^2=0.003u_{in}^2 \text{ and } \varepsilon_{in}=\frac{c_\mu k_{in}^{3/2}}{0.003R}$$

At the Axis:-
Zero shear stress condition has been taken for the axis.

At the Wall:-

(a) No slip wall boundary condition has been taken for the solid wall (u = v = w = 0).

(b) Both *k* and ε are handled by the wall function.

At the Outlet:-

Fully developed flow condition has been taken at the outlet. (i.e. $\frac{\partial \phi}{\partial x} = 0$)

5. VALIDATION OF THE PRESENT NUMERICAL METHOD

In figure 2 the variation of the reattachment length with the swirling angle has been plotted. The benchmark experimental results of Lilley [7] and numerical results of Chuang *et al* [15] are plotted along with results obtained from the present calculations. By measuring the time-mean velocity in the confined swirling flow using Five-hole pitot probe, Lilley [7] presented the experimental results for the inlet swirling angle of 0, 15 and 45 degrees respectively. Chuang *et al* [15] got the numerical result by applying the non-uniform grid system with 58 × 31 grid points. The results of Chuang *et al* [15] were for the inlet swirling angle of 0, 15 and 45 degrees respectively. The inlet swirling angles for the present calculation are 0, 15, 45, 60 and 75 degrees respectively. In the present analysis the uniform grid system with 251 X151 points has been applied.

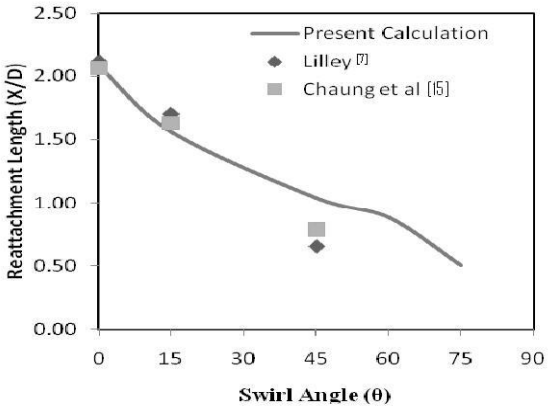

Fig 2. Variation of reattachment length with respect to swirling angles

From the above figure it is observed that for the non-swirling condition i.e., when the inlet swirling angle and the swirl number is zero, the reattachment length calculated from the present analysis is almost same as that of the experimental analysis of Lilley [7] and the numerical analysis of Chuang *et al* [15].

In between the inlet swirling angle 0° to 15° the reattachment length obtained from the three results shows almost the same rate of decrement of the reattachment length with the increase in inlet swirling angle. For the swirling angle of 15° the reattachment length from the experimental results is more than the other numerical results. The result of Chuang *et al* [15] for the swirling angle of 15° is approximately equal to the results of the present calculations.

In between the inlet swirling angle 15° to 45° the rate of decrease of the reattachment length with the swirling angle is more for the experimental result than that of the numerical results. The reattachment length obtained from the experimental result is less than the other two numerical results. At the swirling angle of 45° there is small deviation between the experimental analysis results and the numerical analyses results. The rate of decrease of the reattachment length in between 15° and 45° is more linear for the results of Lilley [7] and Chuang *et al* [15]. In present analysis for the inlet swirling angle of 45° the reattachment length (x/D) is 1.04. The reattachment length obtained from the results of Lilley [7] and Chuang *et al* [15] are 0.65 and 0.78 respectively. So for the swirling angle of 45° the reattachment length from the present analysis is greater than the other two results.

In the present analysis the inlet swirling angle upto 75° is considered. In between 45° to 60° the rate of decrease of the reattachment length is steady. In the present calculation the reattachment length (x/D) at the inlet swirling angle 60° is 0.88. The reattachment length in between 60° and 75° decreases more rapidly than the previous observed intervals of the inlet swirling angles. The reattachment length (x/D) at the inlet swirling angle of 75° is 0.50. The results obtained from the benchmark experimental and numerical analyses are found to be in good agreement with the present calculations.

A correlation has been obtained between the reattachment length and the inlet swirl angle which is given below.

Reattachment Length (L_R) = - 0.019θ + 1.976

From the correlation it is possible to estimate roughly the recirculation size changes with the swirling angle. It can be concluded from the above that for the same Reynolds number and the expansion ratio the reattachment length decreases with the swirling angle or the swirl number.

6. RESULTS AND DISCUSSIONS

The effects of the swirl on the recirculation bubble are analyzed by varying the inlet swirl angle. The inlet swirl angle is varied keeping the geometry of the circular passage constant. The diameter of the circular passage at the upstream is 0.0625 m. The downstream diameter of the circular passage is 0.125 m. The length of the passage at the upstream is 0.04 m. The downstream length of the circular passage is 0.75 m. The expansion ratio i.e. the ratio between the diameter of the circular passage at the downstream and the diameter of the circular passage at the upstream for the present analysis is taken as 2. The axial inlet velocity considered for the analysis is 15 m/s. The Reynolds number for the analysis is 1.26×10^5, it is based on the axial bulk inlet velocity at the upstream. The geometric parameters, axial inlet velocity, expansion ratio and Reynolds number remains constant throughout the present analysis. The inlet swirling angles considered for the analysis are 0, 15, 45, 60 and 75 degrees respectively. The corresponding swirl numbers are 0, 0.18, 0.67, 1.16 and 2.49 respectively. The tangential velocity depends on the inlet swirling angle so with the change of the inlet swirling angle the tangential velocity also changes. The tangential velocities for the inlet swirling angles 0, 15, 45, 60 and 75 degrees are 0 m/s, 4

m/s, 15m/s, 26 m/s and 56 m/s respectively.

The streamline contour, flooded contour and vector plots are utilized to illustrate the effects of the recirculation bubbles on the main flow. The reattachment length or the recirculation bubble lengths for different swirling angles or swirl numbers are obtained.

In the fig. 3 the effects of the swirl number on the recirculation bubble have been shown in streamline and flooded contour plots and in fig.4 the effects of the same parameter on the recirculation bubble have been shown in vector diagram. In both the figures the first streamline and contour plot and vector diagram are obtained respectively for the inlet swirling angle of 0°. The corresponding swirl number for the first plot is zero. The zero swirl number represents the non-swirling flow. The next four plots of both the above respective figures are for the inlet swirling angle greater than zero, so that plots are obtained for the swirling condition. The recirculation bubble is generated in the corner of the passage. For the non-swirling flow condition from the first plot of the above figures it is observed that the size and strength of the recirculation bubble is more than the swirling condition. From the vector diagram of the fig.4 it is observed that the flow in the recirculation region is in the anti-clockwise direction.

For the second plots of both the figures the inlet swirling angle is increased to 15° keeping the inlet velocity and geometrical parameters constant. The corresponding swirl number also increases to 0.18. In this case also the recirculation bubble is generated at the corner of the passage. From the streamline plots of the figure it is observed that for the swirling condition the dividing streamline is more towards the corner portion of the passage than the non swirling condition. This implies that the size of the recirculation bubble generated for the swirling condition is smaller than the recirculation bubble generated for the non swirling condition. The strength of the recirculation bubble obtained from the swirling condition is less than the non-swirling condition. The flow direction remains same for both the swirling and non-swirling condition.

In the third plots of both the above figures the swirling angle is taken as 45° and the corresponding swirl number is 0.67. The inlet velocity and the geometrical parameters remain same as that of the previous two described cases. With the increase in the swirl number the dividing streamline moves toward the corner portion of the passage. Here in this case size and the strength of the generated recirculation bubble is further smaller than the previous two cases. The direction of the flow in the recirculation region remains same as that of the previous cases.

For the forth plot of both the above respective figures the considered inlet swirl angle is 60° keeping the axial inlet velocity and geometric parameters as same as that of the previous cases. The corresponding swirling number is 1.16. With increase in the swirl number to 1.16 the reattachment point further moves towards the corner of the passage. The recirculation bubble generated in the passage for the above swirl number is much smaller than the previous three cases.

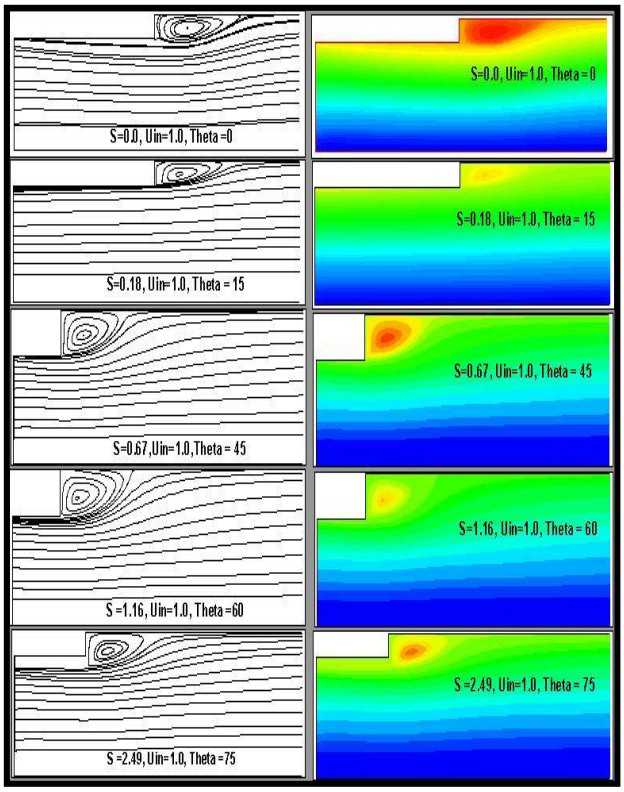

Fig 3. Effect on recirculation size with the variation of swirling number

In the fifth plots of both the above figures the inlet swirling angle is increased to 75°. The other parameters are considered same as that of described in the previous cases. The swirl number for this swirling angle is 2.49. Here in this case also the dividing streamline and the reattachment point shifts towards the corner of the passage with increase in the swirl number. This shows that the recirculation bubble obtained in this case is of smaller size and strength than the other four previous cases. From the above vector diagram it is found that the flow direction in the recirculation region remains same in all the cases.

From the streamline plots of the fig. 3 it is observed the dividing streamline and the reattachment point moves more towards the corner of the passage with the increase in the swirl number. Here the shifting of the reattachment point towards the corner of the passage implies that the size and shape of the recirculation zone decreases with the increase in the swirling number or the swirling angle. For the non-swirling flow condition the size of the recirculation zone generated at the corner of the passage is much greater than the recirculation bubble generated for the swirling condition. It is observed that with the increase in the swirling number the recirculation bubble size decreases. The swirl number represents the swirling strength. From streamline and flooded contour plots of the above figure it is found that the swirling strength has a strong effect on the flow field. With increase in the swirl number the flow field becomes more stabilized. Therefore we can conclude that the swirl has the stabilizing effect on the recirculation bubble.

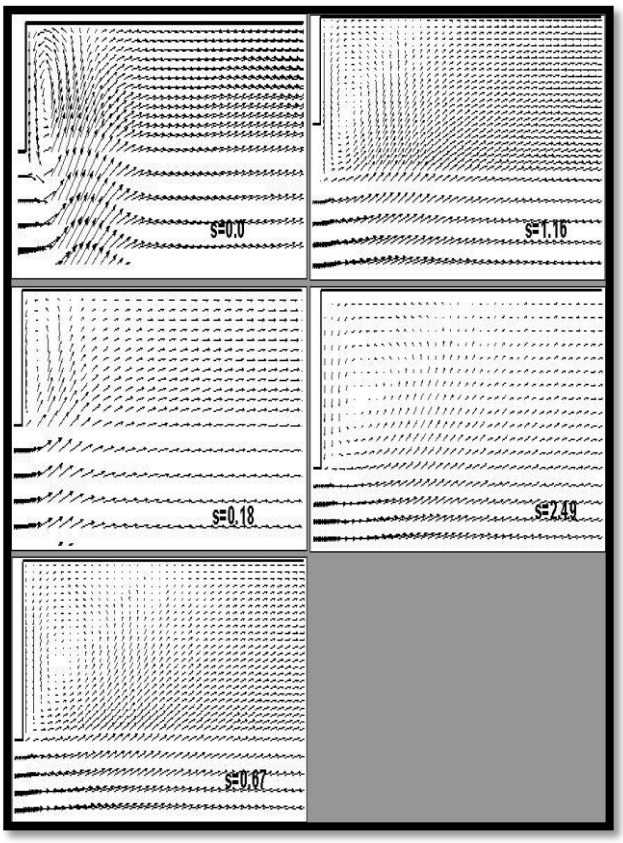

Fig 4. Effect on recirculation size with the variation of swirling number

The turbulent kinetic energy is increased by means of the swirling effect. The swirling flow increases the turbulent mixing. The turbulent mixing enhances the uniform distribution of the temperature in the combustion chamber. Thus the combustion efficiency is increased with the large swirl number.

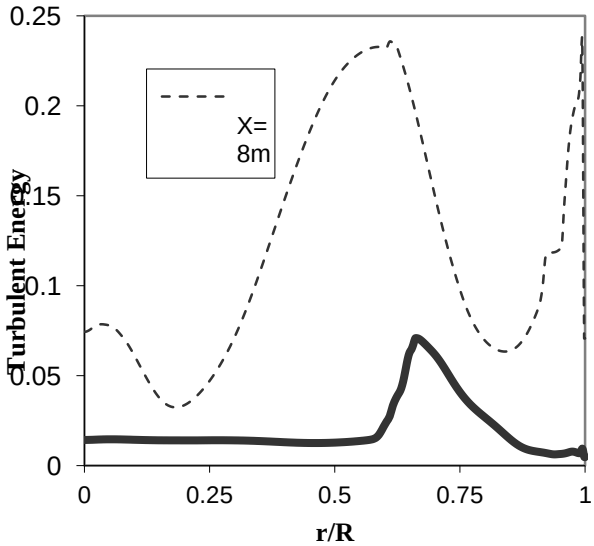

Fig 5. Radial distributions of turbulent energy at x=8 m and x=16 m

In the fig. 5 the radial distributions of the turbulent energy for different axial position have been plotted. The above radial distributions of the turbulent energy are for the expansion ratio of 1.6. In the first case the variation of the turbulent energy has been obtained at the axial position of 8 m from the upstream side of the passage. In this case it is observed that before the recirculation region the variation of the turbulent energy is steady with respect to the radius. The maximum turbulent kinetic energy is in the recirculation region as it is physically expected to be. After that the turbulent energy is in decreasing trend because towards the solid wall there exist the laminar sub layer. We know in a laminar sub layer the flow is no longer turbulent and the turbulent intensity has to be zero at the vicinity of the wall. Hence this drooping nature of the turbulent energy is physically possible. In the second case the distribution of the turbulent energy at the axial position of 16 m from the left side of the passage has been obtained. In this case it is observed that the turbulent energy fluctuates with respect to the radius and the highest turbulent energy is around the recirculation zone. From this we can say that the recirculation zone is the region of highest turbulent in the flow field.

In fig. 6 and 7 the radial distributions of the axial velocity at different axial positions for the expansion ratio of 1.6, have been plotted. In the fig. 6 the axial velocity distribution is obtained at the axial position of 8 m and in fig. 7 the axial velocity distribution for the axial position of 16 m. The existence of the recirculation region is observed in both the cases by the flow reversal. At the axial position of 8 m the negative axial velocity is found to be more than the negative axial velocity distribution for axial position of 16 m.

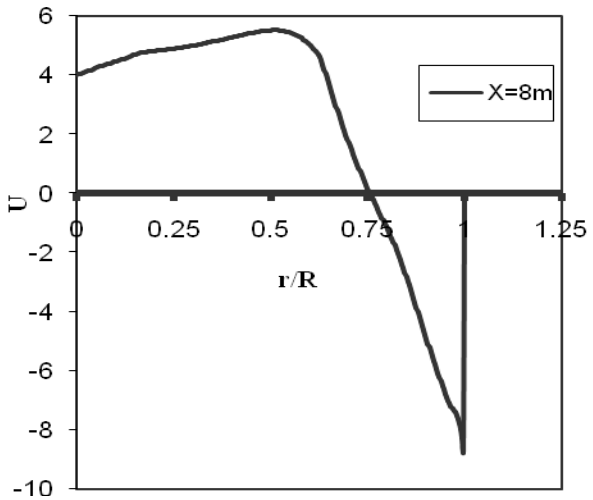

Fig 6. Radial distribution of axial velocity at x=8 m

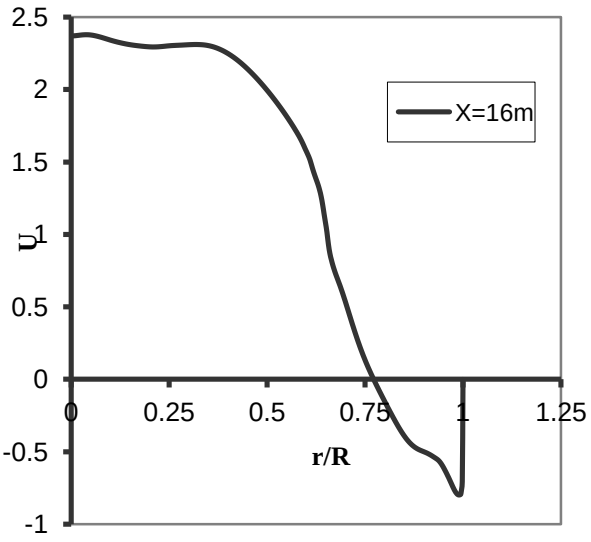

Fig. 7. Radial distribution of axial velocity at x=16 m

From the above figures it is observed that the recirculation zone at the axial position of 16 m is less than the recirculation zone at the axial position of 8 m. The axial position of 8 m is near to the expanded portion of the passage and the axial position of 16 m is further towards the downstream from the expanded portion of the passage. The core of the recirculation zone for the expansion ratio of 1.6 is approximately around the axial position of 8 m. From the axial velocity profiles it can be said that on moving from core of the recirculation zone towards the downstream of the flow field axially the size and effect of recirculation bubble decreases.

7. CONCLUSION

The numerical analysis of the turbulent fluid flow through the sudden expansion passage has been carried out by applying modified k-ε model. The effects of inlet swirl on the recirculation bubble have been investigated. The size and the strength of the recirculation bubble decreases with the increase in the inlet swirl angle or the swirl number. It can be concluded from the above analyses that the swirl has the stabilizing effect on the turbulent flow through the sudden expansion passage. These flow parameters are needed to be controlled for the generation of the recirculation bubble as required for combustion or any other purposes like the chemical processes etc. A correlation has been developed between the reattachment length and the swirling angle.

6. REFERENCES

1. Talbot, L., 1954, "Laminar Swirling Pipe Flow," *ASME J. Appl. Mech*., pp. 1-7.
2. Chaturvedi, M. C., 1963, "Flow Characteristics of Axi-Symmetric Expansion," *Journal. Hydraulic div.Proc., ASCE*, 89: pp. 61-92.
3. White, R. A., 1966, "Effect of Sudden Expansions or Compressions on the Turbulent Boundary Layer," *AIAA Journal*, 4(12): pp. 2232-2234.
4. Etheridge, D. W., and Kemp, P.H., 1978, "Measurements of Turbulent Flow Downstream of a Rearward Facing Step," *Journal of Fluid Mechanics*, 86(2): pp. 545-566.
5. Patankar, S. V., 1981, "Numerical Heat Transfer and Fluid Flow," *McGraw-Hill*, New York.
6. Habib, M. A., and McEligot, D.M., 1982, "Turbulent Heat Transfer in a Swirl Flow Downstream of an Abrupt Pipe Expansion," *International J. Heat transfer, Proceedings of the Seventh International Conference, Munich, West Germany, Paper Fc29*, Hemisphere Publishing Corp., pp. 159-164.
7. Lilley, D. G., and Yoon, H. K., 1983, "Five–hole Pitot Probe Time-mean Velocity Measurements in Confined Swirling Flows," *AIAA Paper*, pp. 83-0315.
8. Aoki, K., Shibata, M., and Nakayama, Y., 1986, "Study on the Flow with a Swirl Flow in a Cylindrical Combustor," *Bulletin of JSME*, 29(258): pp. 4113 - 4121.
9. Hallet, W. L. H., 1988, "A Simple Model for the Critical Swirl in a swirling Sudden Expansion Flow," *Journal of Fluid Engineering*, 110: pp. 155-160.
10. Hallet, W. L. H., and Ding, C. Y., 1995, "A Momentum Integral Model for Central Recirculation in Swirling Flow in a Sudden Expansion," *The Canadian Journal of Chemical Engineering*, 73: pp.284-291.
11. Aloui, F., and Souhar, M., 2000, "Experimental Study of Turbulent Asymmetric Flow in a Flat Duct Symmetric Sudden Expansion," *Journal of Fluids Engineering*, 122: pp. 174-177.
12. Palm, R., Grundmann, S., Weismüller, M., Šaric, S., Jakirlic, S. and Tropea, C., 2006, "Experimental Characterization and Modelling of Inflow Conditions for a Gas Turbine Swirl Combustor," *International Journal of Heat and Fluid Flow*, 27(5): pp. 924-936.
13. Vanierschot, M., and Van den Bulck, E., 2008, "The Influence of Swirl on the Reattachment Length in an Abrupt Axi-symmetric Expansion," *International Journal of Heat and Fluid Flow*, 29: pp. 75–82.
14. Launder, B.E., and Spalding, D.B., 1974, "the Numerical Computation of Turbulent Flows", *Computer Methods in Applied Mechanics and Engineering*, 3: pp. 269-289.
15. Chuang, SH., Lin, HC., Tai, FM and Sung HM., 1992, "Hot flow analysis of swirling sudden-expansion dump combustor," *International Journal of numerical Methods in Fluids*, 14: 217-239.

7. NOMENCLATURE

Symbol	Meaning	Unit
C_{s1}	Empirical Constant	-
C_{s2}	Empirical Constant	-
C_{μ}	Empirical Constant	-
$\bar{u}$	Time mean velocity along Z axis.	(m/s)
$\bar{v}$	Time mean velocity along r axis	(m/s)
u_{in}	Average inlet velocity	(m/s)
	Swirl Number	-

S	Rate of Production	-
G	Turbulent kinetic energy	(m^2/s^2)
k	Radial co-ordinate across the duct	-
r	Length at the down stream	(m)
L	Length at the upstream	(m)
L_i	Reattachment length	(m)
L_R	Radius at inlet	(m)
r_i	Reynolds number	-
Re	Axial co-ordinate along the duct	-
Z	Molecular or laminar viscosity	$(N\text{-}s/m^2)$
μ_l	Turbulent viscosity	$(N\text{-}s/m^2)$
μ_t	Effective viscosity	$(N\text{-}s/m^2)$
μ_{eff}	Turbulence kinetic energy dissipation rate	(m^2/s^3)
ε	Prandtl number of the turbulent kinetic energy	-
σ_k	Dissipation Energy	-
σ_ε	Density	(Kg/m^3)
$\boldsymbol{\rho}$		

8. MAILING ADDRESS

Dr. Snehamoy Majumder
Associate professor
Department of Mechanical Engineering
Jadavpur University, Kolkata- 700032
West Bengal, INDIA.
Phone: 09831369134(mob)
Email ID: srg_maj@yahoo.com